



A social theory-enhanced graph representation learning framework for multitask prediction of drug–drug interactions

Yue-Hua Feng , Shao-Wu Zhang, Yi-Yang Feng, Qing-Qing Zhang, Ming-Hui Shi and Jian-Yu Shi 

Corresponding authors. Shao-Wu Zhang, E-mail: zhangsw@nwpu.edu.cn; Jian-Yu Shi, E-mail: jianyushi@nwpu.edu.cn

Abstract

Current machine learning-based methods have achieved inspiring predictions in the scenarios of mono-type and multi-type drug–drug interactions (DDIs), but they all ignore enhancive and depressive pharmacological changes triggered by DDIs. In addition, these pharmacological changes are asymmetric since the roles of two drugs in an interaction are different. More importantly, these pharmacological changes imply significant topological patterns among DDIs. To address the above issues, we first leverage Balance theory and Status theory in social networks to reveal the topological patterns among directed pharmacological DDIs, which are modeled as a signed and directed network. Then, we design a novel graph representation learning model named SGRL-DDI (social theory-enhanced graph representation learning for DDI) to realize the multitask prediction of DDIs. SGRL-DDI model can capture the task-joint information by integrating relation graph convolutional networks with Balance and Status patterns. Moreover, we utilize task-specific deep neural networks to perform two tasks, including the prediction of enhancive/depressive DDIs and the prediction of directed DDIs. Based on DDI entries collected from DrugBank, the superiority of our model is demonstrated by the comparison with other state-of-the-art methods. Furthermore, the ablation study verifies that Balance and Status patterns help characterize directed pharmacological DDIs, and that the joint of two tasks provides better DDI representations than individual tasks. Last, we demonstrate the practical effectiveness of our model by a version-dependent test, where 88.47 and 81.38% DDI out of newly added entries provided by the latest release of DrugBank are validated in two predicting tasks respectively.

Keywords: drug–drug interaction, graph representation learning, Balance theory, Status theory, multitask learning

Introduction

Polypharmacy—also termed as multidrug treatment—is becoming a promising strategy for treating complex diseases (e.g. diabetes and cancer) in recent years [1]. Nevertheless, the joint use of two or more drugs trigger pharmacological changes (named drug–drug interactions) may result in unexpected effects (e.g. side effects, adverse reactions and even serious toxicity) [2]. Therefore, it is crucial to identify drug–drug interactions (DDIs) before making safe polypharmacy. However, this task is still both expensive and time-consuming *in vitro* and *in vivo* due to the vast space of drug pairs. Over the past decade, the build-up of experimentally determined DDI entries enables computational methods, especially machine learning-based methods, to identify the potential DDIs [3].

With the advantages of both high efficiency and low costs, various machine learning methods have been proved as promising methods to provide preliminary screening of DDIs for further experimental validation. Generally, they train models by using the approved DDIs to infer the potential DDIs among massive unlabeled drug pairs. The training involves diverse drug properties, such as chemical structure [4–8], targets [4, 5, 8, 9], anatomical taxonomy [6, 9, 10] and phenotypic observation [7–10]. Earlier methods focus on the mono-type DDI prediction, which just infers whether a drug interacts with another or not. These methods are usually implemented by classical classifiers (KNN [6], SVM [6], logistic regression [4, 10], decision tree [11] and naïve Bayes [11]), network propagation of the reasoning over drug–drug network

structure [10, 12], label propagation [13], random walk [5] and probabilistic soft logic [9, 11] or matrix factorization [7, 8, 14].

Traditional machine learning methods focus on hand-extracted features and model-driven classifier design, whereas the feature extraction process relies heavily on domain knowledge, so traditional machine learning methods are limited in their ability to deal with raw data. Deep learning has achieved initial success in DDI multi-type prediction due to its powerful ability of automatic feature extraction [15–24]. In common, the methods [15–17] first treat rows in a drug similar matrix as corresponding drug feature vectors, and set the concatenation of two feature vectors as the feature vector to represent a pair of drugs, and then train a multilayer DNN with both feature vectors and types of DDIs as the classifier to predict multi-type DDIs. In addition, the methods [18, 21–24] construct graph neural network framework for multi-type DDI prediction. Asada *et al.* [25] utilizes the DDI description of DrugBank and molecular structure for DDIs prediction. GoGNN [22], MR-GNN [23] and SSI-DDI [18] extract drug features from molecular structure graphs. After extracting drug features, GoGNN [22] uses specific relationship matrix to predict multi-type drug interactions and MR-GNN [23] uses a 2-layer MLP to predict multi-types DDIs. Although SSI-DDI [18] contributes little to the improvement of prediction performance, it makes an effort to DDIs interpretability. Moreover, MUFFIN [24] and MIRACLE [23] construct a graph neural network framework by combining DDI network with its molecular structure for multi-type DDI prediction, in which MIRACLE uses the contrastive

learning of mutual information maximization to learn drug features.

Although these methods have achieved inspiring results, they ignore enhancive and depressive pharmacological changes triggered by DDIs. In addition, they neglect the different pharmacological roles of two drugs in an interaction. More importantly, such properties imply significant patterns (e.g. balance and status triads) among DDIs [26]. To address the above issues, we first leverages Balance theory and Status theory from social networks to characterize pharmacological patterns of DDI, and organize DDI entries into a signed and directed network that reflects the relational semantics between drugs [27, 28], where edges with positive sign and negative sign indicate enhancive and depressive pharmacological changes, source nodes and target nodes are influencing drugs and affected drugs, respectively. And then, we design a novel multitask graph representation learning model to capture the task-joint information by integrating relation graph convolutional networks with Balance and Status patterns to predict the enhancive/depressive DDIs and the directed DDIs. Through the Balance theory and Status theory, we can reveal pharmacological interaction patterns in the DDI network, which can help understand the underlying interaction mechanism between drugs.

Materials and methods

Datasets

We built the signed and directed DDI network by collecting DDI entries from DrugBank (31 March 2021; [29]) in the following steps. First, we downloaded the completed XML-formatted database (including the comprehensive profiles of 11 440 drugs), and parsed all approved small-molecule drugs (i.e. 1935 drugs) and their 589 827 DDIs entries.

Then, we organized them into a signed and directed DDI network where nodes are drugs and edges are their interactions, and labeled the sign '+' for enhancive DDIs and the sign '-' for depressive DDIs according to the keywords 'increase' and 'decrease' in interaction statements, respectively. Moreover, we set the influencing drugs as source nodes and the affected drugs as target nodes according to their semantic roles in interaction statements. For example, the interaction statement 'The therapeutic efficacy of Benmoxin can be increased when used in combination with Pregabalin' implies that the enhancive pharmacological change of Benmoxin (the affected drug) has been induced by Pregabalin (the influencing drug). Thus, the interaction between Pregabalin and Benmoxin is labeled as '+' and a directed edge from Pregabalin to Benmoxin. Similarly, the interaction statement 'The absorption of Drug Rosuvastatin can be decreased when combined with Drug Sodium bicarbonate' indicates a depressive interaction between Rosuvastatin and Sodium bicarbonate (denoted sign '-') and a directed edge from Sodium bicarbonate to Rosuvastatin.

There are some issues that need to be stated. The first is about extraction of interaction signs. First, It is much better if the interaction signs are determined based on beneficial or adverse effect of interaction statement semantics in DrugBank, but some DDI statements could clearly tell whether the DDIs are beneficial or adverse in terms of PD properties (e.g. the therapeutic efficacy or adverse effect) and some could not be clearly determined the benefit by their statements if they involve PK properties (e.g. absorption, metabolism, serum concentration and especially drug activity). For instance, the statements 'Sodium bicarbonate can cause a decrease in the absorption of Rosuvastatin', and 'Octreotide may increase the bradycardic activities of Ceritinib'.

We listed 10 interaction statement patterns of DDI-induced activities as examples in Table S2 in Supplementary Data available online. Therefore, we use the keywords of 'increase/decrease' in interaction statements to determine the signs of DDIs, which only reflect their pharmacological enhancive/depressive changes. The second issue is about extraction of interaction directions. We determined influencing/affected roles between all drugs by their interaction sentence patterns in DrugBank. Furthermore, after checking through the 589 827 collected DDI entries, we found no bi-directional interactions between drugs in DrugBank. And we also verified consistent results in other databases, including drugs.com and PubChem. Thus, there is no drug pair with mutual interaction effects in DrugBank. Finally, we obtained a mono-directed DDI network.

The statistical properties (i.e. the number of drugs, the number of interactions, the number of enhancive DDIs, the number of depressive DDIs, average degree and max degrees) of the signed and directed DDI network built in this paper are summarized in Table 1.

Moreover, we also extracted The MACCS fingerprints of drug chemical structures and input them into the Task-joint embedding module of SGRL-DDI along with the DDI network. In details, after extracting the drug chemical structures represented by simplified molecular input line entry system (SMILES) strings from the XML file of DrugBank, we encoded them by MACCSkeys (Molecular ACCess System keys) Fingerprints [30]. Thus, each drug is represented into a 166-dimensional binary vector, in which the elements indicate the occurrence of a set of predefined substructures.

Problem formulation

Suppose n drugs $\mathcal{V} = \{v_i\}$ and m interactions $\mathcal{L} = \{l_{ij}\}$ among these drugs. The traditional DDI prediction and the multitask prediction are the following different scenarios.

- (i) The task of traditional DDI prediction learns a function mapping $\mathcal{F} : \mathcal{V} \times \mathcal{V} \rightarrow \{0, 1\}$ to deduce potential interactions among unlabeled pairs of drugs in \mathcal{V} (Figure 1A).
- (ii) The multitask prediction includes two subtasks, the task of predicting enhancive and depressive pharmacological changes and the task of predicting directed interactions between drugs (Figure 1B). It learns two functions mapping $\mathcal{F}_{sign} : \mathcal{V} \times \mathcal{V} \rightarrow \{r_+, r_-\}$ and $\mathcal{F}_{direction} : \mathcal{V} \times \mathcal{V} \rightarrow \{r_{in}, r_{out}\}$, wherer r_+ and r_- denote the enhancive and depressive changes triggered by an DDI (i.e. $v_i - v_j$, or $v_i + v_j$), and r_{in} and r_{out} denote the directed relations between two interacting drugs (i.e. $v_i \rightarrow v_j$, or $v_i \leftarrow v_j$), respectively.

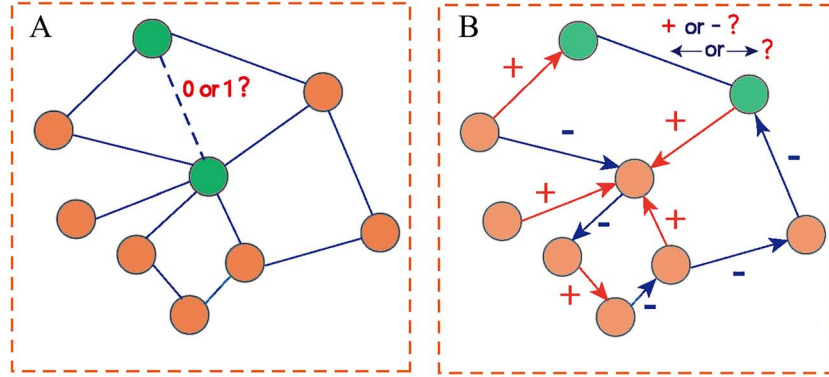
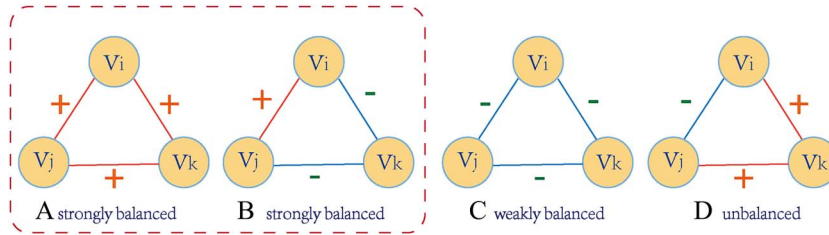
Balance theory and Status theory

Balance theory and Status theory are classical sociological theories that play an essential role in analyzing and modeling signed and directed graphs. According to Balance theory, the positive sign of an edge represents trust, like and approval relationship, whereas the negative sign indicates hostility, distrust, hate and disapproval relationship between two nodes in social networks [31]. In addition, the directed edge between nodes also reflects different relations and semantics [27, 32]. For example, in a directed social network, nodes having many incoming edges and few outgoing edges are termed as celebrities, and in contrast, nodes having few incoming edges and many outgoing edges are termed as followers [33]. Analogous to drugs, celebrities are influencing

Table 1. Statistical properties of the signed and directed DDIs network

# Drug	# Interaction	# Enhancive DDIs	# Depressive DDIs	Average degree	Max degree	
					In_degree	Out_degree
1935	589 827	295 495	294 332	305	1274	1047

Denotes the number.

**Figure 1.** Two DDI prediction scenarios. (A) Traditional DDI prediction. (B) Multitask prediction (i.e. pharmacological changes and directed relation).**Figure 2.** Four types of triads in a signed network. (A) and (B) Strongly balanced. (C) Weakly balanced. (D) Unbalanced.

drugs, whereas followers are affected drugs in interactions. Status theory extends the application of balance theory to signed directed network. It supposes directed relationship labeled by a positive sign '+' or negative sign '-' means target node has a higher or lower status than source node [34].

Therefore, in the signed and directed DDIs network, we use the positive or negative sign to denote enhancive or depressive pharmacological change and the direction to indicate the asymmetrical relation between two interacting drugs of a DDI. We used a signed and directed network to represent the comprehensive DDIs, and employed these social theories to extract topology feature of the DDIs network. In this section, we will briefly introduce these two theories.

Balance theory is widely used to determine how balanced a signed network is [35]. As shown in Figure 2A and B, triangle patterns (i.e. triads) represent the relations between three nodes in a signed graph, where an even number of negative edges are taken as the strong balanced [36]. For a toy example, Figure 2A and B illustrate the strong balanced triads. Figure 2C is a weak balanced triad according to the weak Balance theory [37], whereas Figure 2D shows an unbalanced triads. Specifically, strong balanced triads exemplify the principle that a person is also my friend if he/she is my friend's friend, and a person is my enemy if he/she is my friend's enemy. If the number of strong triads is significantly more than the number of other triads, the signed network is called balanced.

The Status theory is an extension of the Balance theory in the case of networks with both signs and directions. It supposes that if

there is a positive link from node v_i to node v_j , then v_j is considered to have a higher social status than v_i . Also, if there is a negative link from v_i to v_j , then v_i is considered to have a higher social status than v_j . In other words, we can formulate the Status theory as that if $v_i \xrightarrow{+} v_j$, then $S_{v_i} < S_{v_j}$, and if $v_i \xrightarrow{-} v_j$, then $S_{v_i} > S_{v_j}$, where S_{v_i} denotes the status score of v_i . In social networks, the status may indicate relative prestige or reputation. There are totally 12 triads in a signed and directed network. For short, we illustrated four cases in Figure 3, where the triads in Figure 3A and B satisfy the Status theory, whereas the triads in Figure 3C and D do not. Similarly, if the number of status triads is significantly more than the number of other triads, the signed and directed network meets the Status theory. In the context of the DDI network, we also verified it meets both the Balance theory and Status theory in Section 'Balance and Status triad statistics', and these patterns can improve the representation of DDI.

SGRL-DDI model

We propose a multitask learning framework SGRL-DDI to deal with two tasks, including the prediction of enhancive/depressive DDIs and the prediction of directed DDIs. SGRL-DDI mainly consists of two modules (Figure 4). The first module is Task-joint embedding, which is composed of a two-layer embedding and an extra enhancer based on social theory. Each embedding layer is constructed by a multi-relation GNNs [38, 39] and a two-layer MLP (multilayer perception) to represent drugs in DDIs network in two tasks simultaneously, whereas the status-based enhancer

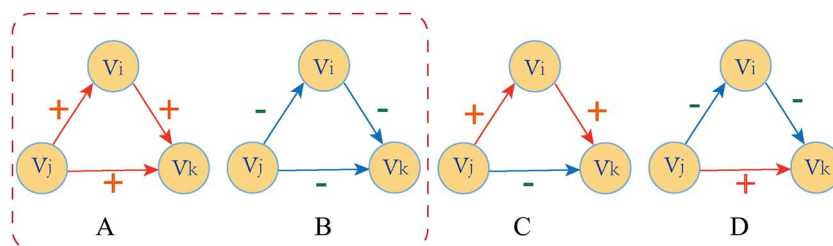


Figure 3. Four types of triads in a signed and directed network. (A) and (B) satisfy the Status theory. (C) and (D) do not satisfy the Status theory.

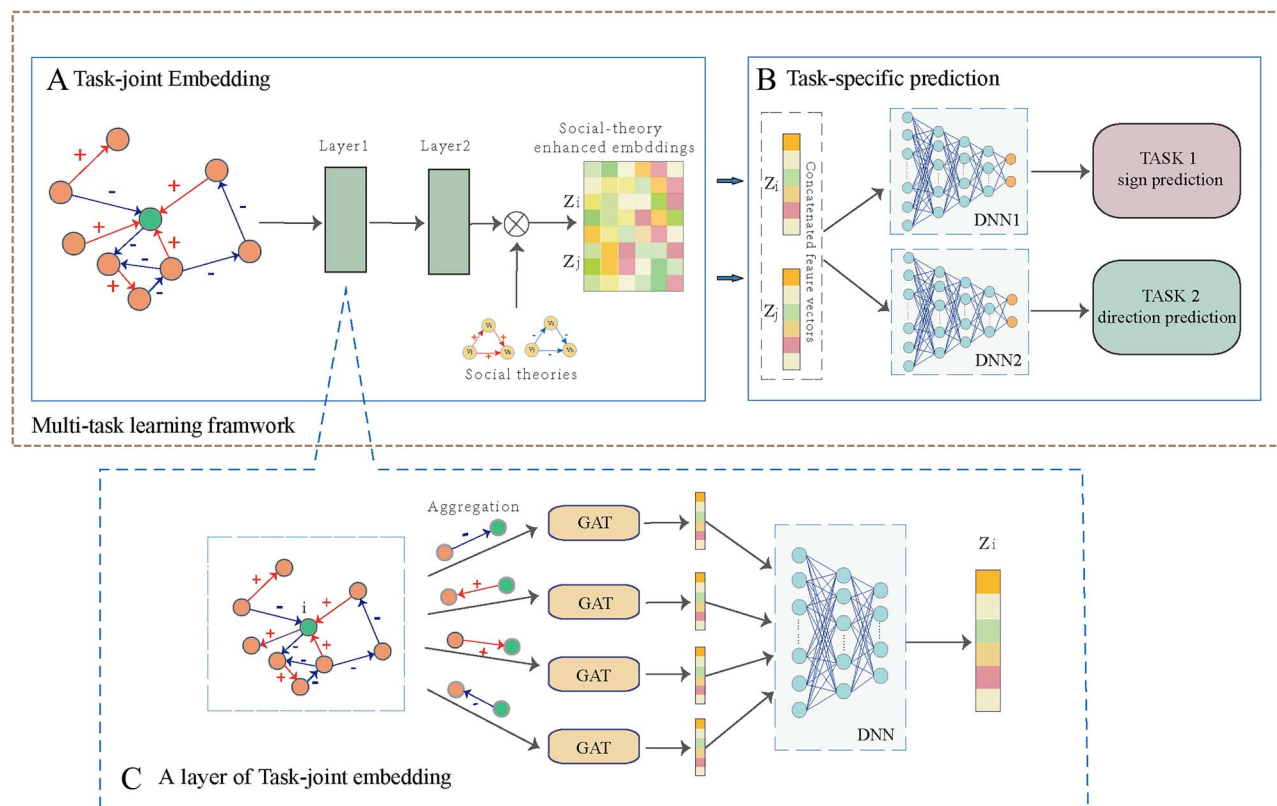


Figure 4. The overall framework of SGRL-DDI. (A) Task-joint embedding module. The two-layer multi-relation GNNs enhanced by Balance and Status theories are built to encode drugs in the DDIs network into feature vectors Z , which captures topological properties of the network combining with both information of signs and directions. (B) Task-specific prediction module. Concatenating two drug latent features to feed into two dense DNNs for implementing two prediction tasks. (C) Illustration of an embedding layer in task-joint embedding module. A central node (i.e. green node) aggregates both the features of its first-order neighbor nodes (i.e. orange) and that of its own separately from different relations (i.e. $v_i \xrightarrow{+} v_j, v_i \xrightarrow{-} v_j, v_i \xrightarrow{+} v_j$ and $v_i \xrightarrow{-} v_j$) to update its features z_i . Then, all the updated features are concatenated to feed into a two-layer DNN for generating the final embedding z_i of node v_i .

enforces the drug task-joint embedding to follow the Balance theory and the Status theory (Figure 4A). The second module is a task-specific prediction (Figure 4B), in which the concatenation vectors of two drug latent features are fed into two dense DNNs to achieve two tasks of predicting enhance/depressive DDIs and predicting the directed DDIs. In SGRL-DDI model framework, the task-joint features of drugs characterize the complementary information of the two tasks, whereas the task-specific dense DNNs capture their exclusive information.

Task-joint embedding module

We use a graph $G(\mathcal{V}, \mathcal{E})$ to represent the signed and directed DDIs network, where $\mathcal{V} = \{v_1, v_2, \dots, v_n\}$ is the set of drug nodes, $\mathcal{E} = \{(v_i, r, v_j)_{i,j=1}^n, r \in R\}$ is the triple set of comprehensive interactions between drug nodes (Figure 4A), and $R = \{r_{\pm}, r_{\mp}, r_{\pm}, r_{\mp}\}$ is the interaction type set with signs and directions ($v_i \xrightarrow{+} v_j, v_i \xrightarrow{-} v_j$,

$v_i \xrightarrow{+} v_j$, and $v_i \xrightarrow{-} v_j$). For example, the triplet (v_i, r_{\pm}, v_j) denotes the interaction from drug v_i to drug v_j with sign '+'. Thus, except for indicating interaction occurrence in the binary DDI network, these edges contain signs and directions between drug nodes.

To propagate and aggregate information on such signed and directed DDIs network, we designed a task-joint embedding module, in which each layer contains four parallel GATs and a two-layer MLP. These GATs account for four relation triples (i.e. $v_i \xrightarrow{+} v_j$, $v_i \xrightarrow{-} v_j$, $v_i \xrightarrow{+} v_j$ and $v_i \xrightarrow{-} v_j$) for propagating and aggregating information for each drug from its different relational neighbors, respectively. The MACCSkeys fingerprints of drug chemical structures are taken as original node features $h_i^{(0)}$ in the DDI network. Formally, the general propagation rule is defined as:

$$h_i^{(k+1)} = \sigma \left(\sum_{j \in N_i^r} \alpha_{ij}^r \mathbf{w}^{r(k)} h_j^{(k)} + \mathbf{w}^{r(k)} h_i^{(k)} \right) \quad (1)$$

where N_i^r denotes the set of v_i 's neighbors in relation r ($r \in R$), $h_i^{(k)}$ is the feature vectors from the layer k , $\mathbf{W}_r^{(k)}$ is the trainable weight matrix of relation r and σ is a nonlinear element-wise activation function (i.e. ReLU). Moreover, α_{ij}^r is the weight value between drug v_i and drug v_j in relation r accumulated by attention mechanism defined as:

$$\alpha_{ij}^r = \text{softmax}(e_{ij}) = \frac{\exp(e_{ij})}{\sum_{k \in N_i^r} \exp(e_{ik})} \quad (2)$$

$$e_{ij} = \text{LeakyReLU} \left(\bar{\mathbf{a}}_r^T \left[\mathbf{W}_{\text{att}}^r h_i^{(1)} \parallel \mathbf{W}_{\text{att}}^r h_j^{(1)} \right] \right) \quad (3)$$

where **LeakyReLU** is nonlinearity activation function (with negative input slope $\alpha=0.2$), " \parallel " is the concatenation operation, $\mathbf{W}_{\text{att}}^r \in \mathbb{R}^{F \times F'}$ is the weight matrix parameter, $\bar{\mathbf{a}}_r \in \mathbb{R}^{2F'}$ is a shared attention weight parameter vector denoted by a single-layer feed-forward neural network, and T denotes transposition operator. For each relation, we obtained the embedding feature vector $h_i^{r(k+1)}$ for drug v_i .

In addition, the two-layer MLP accounts for the integration of four triple representations to generate the integrated embedding vector $h_i^{(k+1)}$ of drug v_i (Figure 4C). It works as an adhesive to extract task-joint embeddings.

$$h_i^{(k+1)} = \mathbf{W}_{m2}^{(k+1)} \left(\mathbf{W}_{m1}^{(k+1)} \left(h_i^{r1(k+1)} \parallel h_i^{r2(k+1)} \parallel h_i^{r3(k+1)} \parallel h_i^{r4(k+1)} \right) \right) \quad (4)$$

where $\mathbf{W}_{m2}^{(k+1)}$ and $\mathbf{W}_{m1}^{(k+1)}$ are the trainable weight matrix in the $(k+1)$ -th layer of the MLP.

Finally, the task-joint embedding module adopts two sequential layers to enhance the nonlinear representation of signed and directed interactions (denoted as $Z_i \in \mathbb{R}^{1 \times H_2}$ in Figure 4).

Social theory-enhanced loss functions in task-joint embedding

Corresponding to the components in the task-joint embedding module, we considered three losses. The first one is traditional loss function L_{network} (i.e. cross-entropy loss) for reconstructing the DDIs network, which measures the difference between the original network G and the reconstructed network \tilde{G} .

$$L_{\text{network}}(v_i, v_j) = - \sum_{v_i, v_j \in E} y_{ij} \log(p(v_i, v_j)) + (1 - y_{ij}) (1 - \log(p(v_i, v_j))) \quad (5)$$

where y_{ij} is the true sign label of edge (v_i, v_j) for the pair of drugs v_i and v_j , E is the set of edges between drug nodes representing DDI, $p(v_i, v_j) = \sigma(\mathbf{z}_i \cdot \mathbf{z}_j^T)$ is the predicting probability computed by the inner product of feature vectors of two drugs that have a link in DDI network, σ is the sigmoid function, and the feature vectors Z is generated by the task-joint embedding.

Since it is expected that the reconstructed network follows the balance theory and state theory, the other two losses account for direction patterns and sign patterns among in interaction triads. That is, the second loss function $L_{\text{direction}}$ (i.e. square loss) measures the difference between the modified reduction $q(v_i, v_j)$ of status-scores of two drugs and their true reduction $(s_{d_i} - s_{d_j})$ [40].

$$L_{\text{direction}}(v_i, v_j) = \sum_{v_i, v_j \in E} \left(q(v_i, v_j) - (s_{d_i} - s_{d_j}) \right)^2 \quad (6)$$

The $q(v_i, v_j)$ is the modified reduction of status-scores of two drugs defined as follows:

$$q(v_i, v_j) = \begin{cases} \max(s_{d_i} - s_{d_j}, 0.5), & \text{if } d_i \rightarrow d_j \\ \min(s_{d_i} - s_{d_j}, -0.5), & \text{if } d_i \nrightarrow d_j \end{cases} \quad (7)$$

where 0.5 is a threshold for separating the nodes with high/low status-scores, and the status score of drug v_i is computed by $s_{d_i} = \text{sigmoid}(\mathbf{W} \cdot \mathbf{z}_i + b)$.

The third loss function L_{triangle} measures how well node triads $\Delta_{(i,j,k)}$ meet the Balance theory.

$$L_{\text{triangle}} = -\log J_{\text{triangle}} = -\sum_{\Delta_{(i,j,k)} \in T} \log(J_{\Delta_{(i,j,k)}}) = \sum_{\Delta_{(i,j,k)} \in T} L_{\Delta_{(i,j,k)}} \quad (8)$$

$$J_{\text{triangle}} = \prod_{\Delta_{(i,j,k)} \in T} J_{\Delta_{(i,j,k)}} \quad (9)$$

$$J_{\Delta_{(i,j,k)}} = f(p(v_i, v_j)) * f(p(v_i, v_k)) * f(p(v_k, v_j)) \quad (10)$$

$$L_{\Delta_{(i,j,k)}} = L_{ij} + L_{ik} + L_{kj}, \text{ and } L_{ij} = y_{ij} \log(p(v_i, v_j)) + (1 - y_{ij}) (1 - \log(p(v_i, v_j))) \quad (11)$$

$$f(p(v_i, v_j)) = \begin{cases} 1 - p(v_i, v_j), & \text{if } d_i \rightarrow d_j \\ p(v_i, v_j), & \text{if } d_i \nrightarrow d_j \end{cases} \quad (12)$$

where $p(v_i, v_j)$ is the predicting probability of edge (v_i, v_j) computed by $\sigma(\mathbf{z}_i \cdot \mathbf{z}_j^T)$, $J_{\Delta_{(i,j,k)}}$ is the balance score of a triad and J_{triangle} is the balance score of the whole network.

Finally, the total loss function of the task-joint embedding module can be formulated as:

$$L_T = L_{\text{network}} + L_{\text{direction}} + L_{\text{triangle}} \quad (13)$$

Task-specific prediction module

Once drug feature vectors containing signs and directions of DDIs are generated by the task-joint embedding module, we concatenated pairwise embedding feature vectors to form the task-joint feature vectors $h(v_i, v_j) = [h_i, h_j]$ of drug pairs.

After obtaining feature vectors of drug pairs, two DNN-based predictors are separately trained for two prediction tasks. In the first prediction task, the positive samples are the edges with the sign '+' and the negative samples are the ones with the sign '-'. In the second prediction task, the positive samples are all edges in the DDIs network, whereas the negative samples are the same drug pairs as the positive samples but with opposite directions. For example, if an interaction is $A \rightarrow B$ labeled as a positive sample, then its directional inverse $A \leftarrow B$ is labeled as a negative sample. Each of the two prediction tasks employs in common a binary cross-entropy loss function $L_P(p, q)$.

$$L_P(p, q) = - \sum_{v_i, v_j \in E} p(v_i, v_j) \log(q(v_i, v_j)) + (1 - p(v_i, v_j)) (1 - \log(q(v_i, v_j))) \quad (14)$$

where $p(v_i, v_j)$ is the true label of the interaction (v_i, v_j) , $q(v_i, v_j)$ is the predicting probability of interaction.

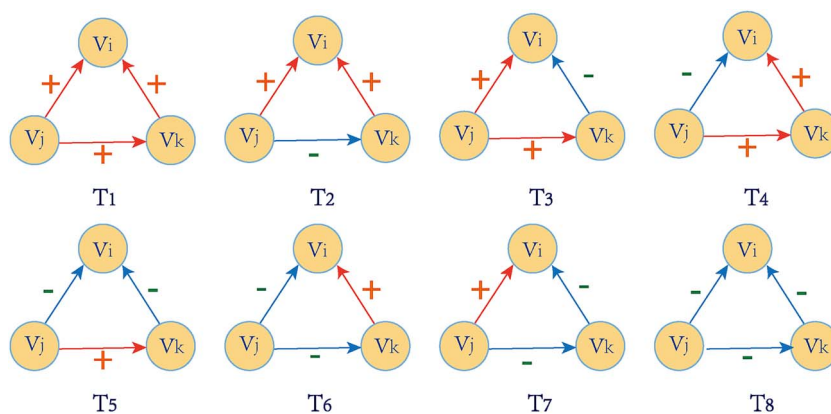


Figure 5. Eight different types of triangles in the signed and directed DDIs network.

Assessment metrics

We randomly partition the dataset into a training set (contains 75% samples), a validation set (contains 5% samples) and a testing set (contains 20% samples). The training set is used to train the model, the validation set is used to tune the parameters of the model, whereas the testing set is used to assess how well the trained model is. The procedure is repeated 10 times, and the average performance is adopted to evaluate the prediction performance of model.

The Accuracy (ACC), Precision, Recall, F1-score, AUC (area under the receiver operating characteristic curve) and AUPR (area under the precision-recall curve) are used to assess the performance of SGRL-DDI. Receiver operating characteristic curve reveals the relationship between true-positive rate (precision) and false-positive rate based on various thresholds. Precision-recall curve reveals the relationship between precision (true-positive rate) and recall based on various thresholds. These metrics are defined as follows:

$$\text{Accuracy} = \frac{TP + TN}{TP + FP + TN + FN} \quad (15)$$

$$\text{Precision} = \frac{TP}{TP + FP} \quad (16)$$

$$\text{Recall} = \frac{TP}{TP + FN} \quad (17)$$

$$F_1 = \frac{2 \times \text{Precision} \times \text{Recall}}{\text{Precision} + \text{Recall}} \quad (18)$$

where TP, FP, TN and FN refer to the numbers of true-positive samples, false-positive samples, true negative samples and false negative samples, respectively. AUC value depends on the average ranks of all true DDIs, whereas AUPR punishes the incorrect predictions of top ranking DDIs more than AUC when the number of negative samples is much larger than the number of positive samples [41].

Results and discussion

In this section, we first revealed the topological patterns and analyzed the signed and directed DDIs network to verify whether it meets the Balance theory and Status theory. Then, we compared our model with the state-of-the-art methods that are usually applied in social networks for both the sign prediction and the direction prediction. After that, we performed ablation studies to verify whether Balance and Status patterns help characterize the signed and directed pharmacological DDIs, and the joint of

two tasks provides better DDI representations than individual tasks. Eventually, we tested our SGRL-DDI with newly added entries in latest release of DrugBank both for two predicting tasks, respectively.

Balance and Status triad statistics

Balance theory and Status theory are two core sociological theories that play an essential role in modeling signed and directed networks. The Balance theory reflects the relationship of triangular structures (triads), whereas the Status theory models the directed relationship between two nodes. In the context of the signed and directed DDI network, there are 26 475 975 triads in total, which are grouped into eight types shown in Figure 5. According to Balance theory and Status theory, we counted how many triads are of strong balance patterns, weak balance patterns and how many triads meet status patterns (Table 2). The proportional distribution of different patterns is shown in Figure 6.

As observed, only in the case of strong balance, $\sim 23.6\%$ of triads satisfy Balance theory, and 67.8% satisfy Status theory (Figure 6A). If the weak balance is considered as a balance, $\sim 82.3\%$ of triads can be consistent with both theories (Figure 6B). Meanwhile, only a tiny number of triangles (0.028%) meet neither the Balance theory nor the Status theory. Therefore, the signed and directed DDI network is similar to the social networks, which meets both the Balance theory and the Status theory. Integrating these two theories with GNNs can represent signed and directed DDIs better.

Performance of SGRL-DDI in sign prediction

In order to validate the performance of SGRL-DDI in sign interaction prediction, we compared SGRL-DDI with other three baseline methods of GCN [42], SNEA [43] and SGCN [44]. The GCN [42] is one of the outstanding graph representation learning methods for binary networks. It maps drug nodes of the network into a latent space to obtain their latent feature vectors for capturing the topological relationship from its neighborhood drugs. Both SNEA [43] and SGCN [44] consider that negative sign links not only have different semantic meanings compared with positive sign links, but also their principles are inherently different. Therefore, these two methods extended the graph representation learning of unsigned networks to that of signed ones. First, they employed Balance theory to aggregate and propagate information for each node from its neighboring nodes that are connected by different sign types of links. Then they used a logic regression as the binary classifier to train and classify the positive signs and negative signs for links. Differently, SNEA [43] leveraged GATs with a self-attention mechanism, whereas SGCN [44] utilized standard GCNs

Table 2. Statistics on Balance and Status theories in the signed and directed DDIs network

Triad label	#Triad	Proportion	Strong balance	Weak balance	Status
T1	2 266 017	0.086	✓	✓	✓
T2	825 613	0.031	×	×	✓
T3	1 588 429	0.060	×	×	✓
T4	747 020	0.028	×	×	×
T5	2 296 230	0.087	✓	✓	✓
T6	1 690 123	0.064	✓	✓	✓
T7	1 518 931	0.057	✓	✓	×
T8	15 543 612	0.587	×	✓	✓

#Denotes the number of each type of triad. Proportion denotes the proportion of this triad in all triad. The three remaining columns indicate whether each triad type satisfies the strong Balance, the weak Balance and the Status, respectively. ✓Denotes yes. ×Denotes no.

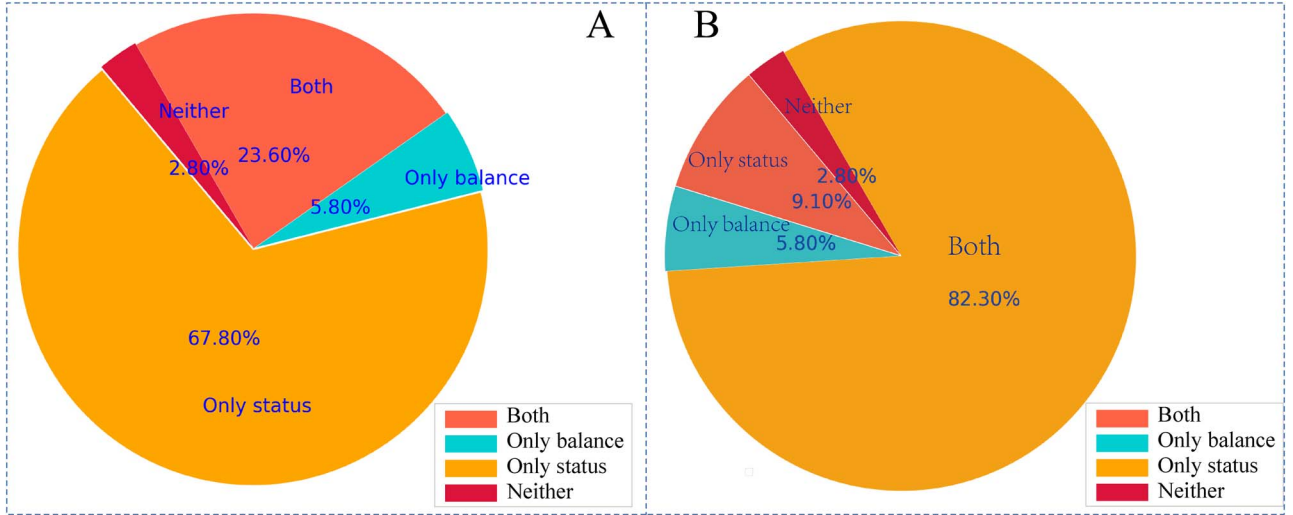


Figure 6. Proportional distribution of triangles satisfying Balance theory and/or Status theory. (A) Statistics without considering weak balance. (B) Statistics with considering weak balance as a kind of balance.

to obtain the latent representation vectors for each node in signed networks.

In the process of sign prediction, enhancive DDIs were considered as positive samples (signed with '+'), and depressive DDIs were labeled as negative samples (signed with '-'). All these samples were split into a training set, a validating set and a testing set. Since GCN is only suitable for unsigned networks, we only took above strategy for validating and testing samples, but made no change on the positive and negative samples of the training set.

In order to learn an optimal model of sign and direction prediction, we tuned the parameters in all the methods. GCN [42], SNEA [43] and SGCN [44] were implemented with their published source codes, and the parameters have been tuned to optimal values. All methods adopt a two-layer GNN, where the dimension of embeddings is 64. In addition, the head number of SNEA is set to 1.

In our SGRL-DDI, the hyper-parameters of the task-joint drug embedding module include learning rate, epochs, batch size, as well as neuron numbers in hidden layers. They are tuned by performing a grid search to the minimum value of the loss functions. The hyper-parameters of the task-specific prediction module are also selected by a grid search to obtain the best prediction results. The optimal values of the hyper-parameters in SGRL-DDI are listed in Table S1, Supplementary Data available online.

The comparison results in Table 3. The raw GCN treats all edges as positive samples and non-DDIs as negative samples. Obviously, it is incapable of discriminating enhancive and depressive interactions since all enhancive and depressive interactions are positive

samples in the training process. A very low precision (0.5015) and an extremely high recall (0.9977) jointly reveal this issue and results in AUC = 0.3947 lower than the random guess.

SNEA and SGCN achieve significantly better prediction than GCN due to their characterization of different signs. In contrast, our SGRL-DDI achieves the best performance in predicting enhancive/depressive interactions with the significant improvements of 4.5–6.7%, 5.23–10.8%, 6.14–13.4%, 6.46–9.2%, 7.94–15.3% and 3.25–10.2% against SNEA and SGCN in terms of AUC, AUPR, F1-score, Accuracy, Precision and Recall, respectively. In short, the results demonstrate the superiority of SGRL-DDI in sign prediction.

Performance of SGRL-DDI in direction prediction

In order to evaluate the performance of SGRL-DDI in the directed interaction prediction, we compared it with other four baseline methods of GCN [42], GGCN-s/t [45], GGCN [45] and DGGAN [46]. These three methods for directed link prediction generally learn two embedding vectors for each node, including a source vector for its outgoing links and a target vector for its incoming links. They are summarized as follows.

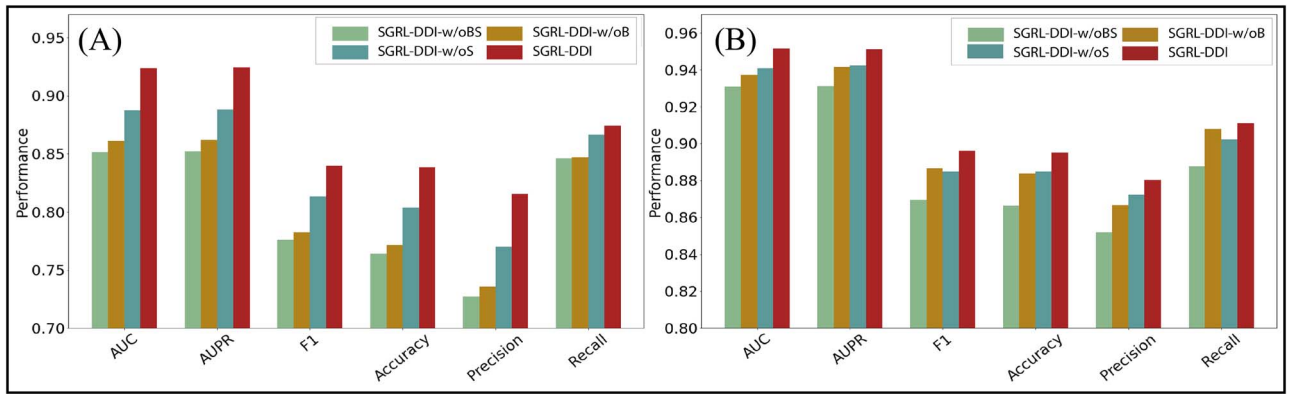
GGCN-s/t [45] measures the likelihood of a link from node i to node j by $\hat{A}_{ij} = \sigma(z_i^{(s)} z_j^{(t)T})$ and the likelihood of a link from node j to node i by $\hat{A}_{ji} = \sigma(z_j^{(s)} z_i^{(t)T})$, where $z_i^{(s)}$ is the source vector and $z_i^{(t)}$ is the target vectors. The bigger likelihood determines the direction of the edge (v_i, v_j) . DGGAN [46] uses adversarial mechanisms to deploy a discriminator and two generators that jointly learn

Table 3. Results of SGRL-DDI and other three methods for sign prediction

Methods	AUC	AUPR	F1	Accuracy	Precision	Recall
GCN	0.3947	0.4358	0.6675	0.5034	0.5015	0.9977
SNEA	0.8845	0.8435	0.7656	0.8030	0.7272	0.8088
SGCN	0.9069	0.8985	0.8346	0.8304	0.8008	0.8785
SGRL-DDI	0.9515	0.9511	0.8960	0.8950	0.8802	0.9110

Table 4. Results of SGRL-DDI and other four methods for direction prediction

Methods	AUC	AUPR	F1	Accuracy	Precision	Recall
GCN	0.5000	0.5000	0.5000	0.5000	0.5000	0.6670
GGCN-s/t	0.7235	0.7332	0.6942	0.6142	0.5750	0.8757
GGCN	0.6452	0.6460	0.6668	0.5042	0.5024	0.9921
DGGAN	0.6742	0.6760	0.8213	0.8011	0.7497	0.9054
SGRL-DDI	0.9234	0.9243	0.8396	0.8385	0.8157	0.8743

**Figure 7.** Ablation comparison in the signed interaction prediction (A) and in the directed interaction prediction (B).

each node's source and target vectors. For a given node, the two generators are trained to generate its fake target neighbor nodes and source neighbor nodes from the same underlying distribution, whereas the discriminator aims to distinguish whether a neighbor node is real or fake. GGCN [45] computes the acceleration value of each node embedding to indicate the likelihood that node i is connected to node j in the directed graph, and integrates the acceleration values of nodes and node embeddings to build up an asymmetric graph decoding scheme.

In the directed interaction prediction, all DDIs in the network are considered the positive samples. For each positive sample (v_i, v_j) (i.e. a directed edge from node v_i to node v_j), we form its reverse edge (v_j, v_i) as the corresponding negative sample. All these positive and negative samples are randomly split into a training set, a validating set and a testing set. As the GCN is only suitable for unsigned and undirected networks, we only adopted the above strategy for validating and testing samples. GGCN-s/t, GGCN and DGGAN were implemented with their published source codes and the parameters have been tuned to optimal values.

The comparison results (Table 4) of the directed interaction prediction show that the standard GCN has the worst predicting results since it ignores the directions when reconstructing the adjacency matrix from node embeddings. Indeed, due to the symmetric decoder of the inner product $\hat{\mathbf{A}}_{ij} = \sigma(z_i^T z_j) = \sigma(z_j^T z_i) = \hat{\mathbf{A}}_{ji}$, it obtains the same probability between an edge $(v_i \rightarrow v_j)$ and the reverse edge $(v_i \leftarrow v_j)$. As a consequence, as shown in Table 4, standard GCN is incapable of predicting the directed link in the

directed networks, where relationships are not always reciprocal. GGCN-s/t, GGCN and DGGAN achieve significantly better prediction results than GCN, due to their characterization of directed edges. In contrast, our SGRL-DDI achieves the best performance with the significant improvements of 20–27.8%, 19.1–27.8, 1.82–17.3%, 3.74–33.4% and 6.6–31.3% against GGCN-s/t, GGCN and DGGAN methods in terms of AUC, AUPR, F1-score, Accuracy and Precision, respectively. In short, the results demonstrate the superiority of SGRL-DDI in direction prediction.

Ablation study

In this section, we investigated how the Balance theory and Status theory used in the task-joint embedding module improve the performance of SGRL-DDI. We made three ablated versions of SGRL-DDI. The first version of SGRL-DDI (denoted as SGRL-DDI-w/oBS) was implemented by removing both Balance-enhanced and Status-enhanced parts from SGRL-DDI. The second one (denoted as SGRL-DDI-w/oB) was implemented by removing the Balance-enhanced part. The third one (denoted as SGRL-DDI-w/oS) was implemented by removing the Status-enhanced part. SGRL-DDI and its three variants were evaluated both in the signed interaction prediction (Figure 7A) and the directed interaction prediction (Figure 7B).

The results in Figure 7 reveal the following crucial points. (i) SGRL-DDI with both the balance-enhanced part and the status-enhanced part achieves the best prediction, whereas SGRL-DDI-w/oBS without social theory-based enhancer parts gives the worst

Table 5. Results of SGRL-DDI in the signed and directed interaction prediction for newly added DDIs entries

Two tasks	AUC	AUPR	F1	Accuracy	Precision	Recall
Signed DDI	0.9407	0.9423	0.8847	0.8847	0.8722	0.9023
Directed DDI	0.8973	0.8979	0.8233	0.8138	0.7899	0.8765

prediction results. (ii) Both SGRL-DDI-w/oB and SGRL-DDI-w/oS achieve better prediction results than SGRL-DDI-w/oBS, indicating that Balance-enhanced and Status-enhanced parts can improve the prediction performance. In addition, we also see that the results of SGRL-DDI-w/oS is better than that of SGRL-DDI-w/oB for the directed prediction, showing that Balance-enhanced part contributes more than Status-enhanced part for directed DDI prediction. Therefore, the social theory-based enhancer in SGRL-DDI plays a crucial role by capturing topological patterns in the signed and directed DDI network.

Validation of SGRL-DDI tested by newly added DDIs entries

Except for cross-validation, we further made a version-independent test to validate the ability of our SGRL-DDI for predicting the new DDIs with signed and directed interactions. We extracted newly added interaction entries (i.e. 61 740 DDIs) from the latest release of DrugBank (version 5.1.8, 20 September 2021), and took these new DDIs as the independent testing set. The dataset collected from the previous release of DrugBank (31 March 2021) was taken as the training set (Section 'Datasets') to train our model. The performance of SGRL-DDI is investigated in the tasks of the signed and the directed interaction predictions, respectively.

The results in Table 5 show that SGRL-DDI is adequate for both signed interaction prediction and directed interaction prediction of newly added DDI entries.

To investigate the potential biases of identifying enhancive/depressive DDIs and affected/influencing drugs, we utilized confusion matrices to measure the prediction for newly added DDIs entries in two scenarios (Tables S3 and S4, see Supplementary Data available online). Specifically, we obtained the prediction with Sensitivity (TPR) = 0.9023, Specificity (TNR) = 0.8699 in the scenario of signed DDIs while obtaining the prediction with Sensitivity (TPR) = 0.8765 and Specificity (TNR) = 0.7453 in the scenario of directed DDIs. Obviously, most DDI entries can be identified in terms of pharmacological changes and influencing directions. Thus, there is no significant bias.

Conclusions

The interactions between drugs are comprehensive because they trigger enhancive/depressive and directed pharmacological effects. Analogous to social associations between persons, a set of DDI entries can be represented as a signed and directed network, where the enhancive/depressive changes are labeled as the signs of DDI edges, and pharmacological directions are the directions of DDI edges. The underlying topology of the signed and directed DDI network is often ignored in existing DDI works, whereas the topological patterns hidden in the signed and directed DDI network can help reveal the underlying mechanism of DDIs. Thus, here we first leverage the Balance theory and Status theory to uncover DDI interaction patterns, and then design a novel multitask graph representation learning model framework to predict the enhancive/depressive and asymmetric pharmacological effects of DDIs (i.e. the signed and directed DDIs

prediction). SGRL-DDI can capture the task-joint information by enhancing relation GNNs with Balance and Status patterns. Moreover, SGRL-DDI utilizes task-specific DNNs to perform two prediction tasks of sign and direction of DDIs. Experimental results show that our SGRL-DDI is superior to other state-of-the-art methods for DDI multitask prediction. Furthermore, the ablation study verifies how each component in SGRL-DDI contributes to the prediction performance. The prediction results of enhancive, depressive and pharmacological effects of new DDIs demonstrate the effectiveness of SGRL-DDI in real DDI prediction scenario.

Key Points

- We first leverage Balance theory and Status theory to reveal the topological patterns among directed pharmacological DDIs, which are modeled as a signed and directed network.
- We design a novel graph representation learning model named SGRL-DDI to realize the multitask prediction of DDIs, including the prediction of enhancive/depressive DDIs and the prediction of directed DDIs.
- SGRL-DDI can capture the task-joint information by integrating relation graph convolutional networks with Balance and Status patterns.

Supplementary Data

Supplementary data are available online at <http://bib.oxfordjournals.org/>.

Data availability

The datasets generated and analyzed during the current study and the code of SGRL-DDI are openly available at the website of <https://github.com/NWPU-903PR/SGRL-DDI>.

Acknowledgments

We acknowledge anonymous reviewers for the valuable comments on the original manuscript.

Funding

This work has been supported by the National Natural Science Foundation of China (grant numbers, 62173271, 61873202 and 61872297) and Shaanxi Provincial Key R&D Program, China (grant number 2020KW-063).

Ethics approval and consent to participate

No ethics approval was required for the study.

Consent for publication

Not applicable.

References

1. K. I. Cheng F, Barabási AL. Network-based prediction of drug combinations. *Nat Commun* 2019;**10**(1):1197.
2. S. R. Niu J, Mager DE. Pharmacodynamic drug-drug interactions. *Clin Pharmacol Ther* 2019;**105**(6):1395–406.
3. Sun M, Zhao S, Gilvary C, et al. Graph convolutional networks for computational drug development and discovery. *Brief Bioinform* 2020;**21**(3):919–35.
4. Takeda T, Hao M, Cheng T, et al. Predicting drug-drug interactions through drug structural similarities and interaction networks incorporating pharmacokinetics and pharmacodynamics knowledge. *J Chem* 2017;**9**:16.
5. Zhang W, Chen Y, Liu F, et al. Predicting potential drug-drug interactions by integrating chemical, biological, phenotypic and network data. *BMC Bioinform* 2017;**18**(1):18.
6. Andrej K, Polonca F, Brane LE, et al. Predicting potential drug-drug interactions on topological and semantic similarity features using statistical learning. *Plos One* 2018;**13**(5):e0196865.
7. Yu H, Mao KT, Shi JY, et al. Predicting and understanding comprehensive drug-drug interactions via semi-nonnegative matrix factorization. *BMC Syst Biol* 2018;**12**(Suppl 1):14.
8. Wen Z, et al. SFLN: a sparse feature learning ensemble method with linear neighborhood regularization for predicting drug-drug interactions. *J Inf Sci* 2019;**497**:189–201.
9. Sridhar D, Fakhraei S. A probabilistic approach for collective similarity-based drug-drug interaction prediction. *Bioinformatics* 2016;**32**(20):3175–82.
10. Gottlieb A, Stein GY, Oron Y, et al. INDI: a computational framework for inferring drug interactions and their associated recommendations. *Mol Syst Biol* 2012;**8**(1):8–592.
11. Cheng F, Zhao Z. Machine learning-based prediction of drug-drug interactions by integrating drug phenotypic, therapeutic, chemical, and genomic properties. *J Am Med Inform Assoc* 2014;**21**(e2):e278–86.
12. Feng YH, Zhang SW, Shi JY. DPDDI: a deep predictor for drug-drug interactions. *BMC Bioinform* 2020;**21**(419).
13. Zhang P, Wang F, Hu J, et al. Label propagation prediction of drug-drug interactions based on clinical side effects. *Sci Rep* 2015;**5**(1):12339 2015/07/21.
14. Rohani N, Eslahchi C, Katanforoush A. ISCMF: integrated similarity-constrained matrix factorization for drug-drug interaction prediction. *Netw Model Anal Health Inform Bioinform* 2020;**9**(1):1–8.
15. Ryu JY, Kim HU, Lee SY. Deep learning improves prediction of drug-drug and drug-food interactions. *Proc Natl Acad Sci U S A* 2018;**115**(18):E4304–11.
16. P. C. Lee G, Ahn J. Novel deep learning model for more accurate prediction of drug-drug interaction effects. *BMC Bioinform* 2019;**20**:415.
17. Deng Y, Xu X, Qiu Y, et al. A multimodal deep learning framework for predicting drug-drug interaction events. *Bioinformatics* 2020;**36**(15):4316–22.
18. Nyamabo AK, Yu H, Shi JY. SSI-DDI: substructure-substructure interactions for drug-drug interaction prediction. *Brief Bioinform* 2021;**22**(6):bbab133.
19. Zitnik M, Agrawal M, Leskovec J. Modeling polypharmacy side effects with graph convolutional networks. *Bioinformatics* 2018;**34**(13):i457–66.
20. Yu Y, Huang K, Zhang C, et al. SumGNN: multi-typed drug interaction prediction via efficient knowledge graph summarization. *Bioinformatics* 2021;**37**(18):2988–95.
21. H. Wang, et al., GoGNN: graph of graphs neural network for predicting structured entity interactions, *Twenty-Ninth International Joint Conference on Artificial Intelligence and Seventeenth Pacific Rim International Conference on Artificial Intelligence IJCAI-PRICAI-20*, Yokohama Japan, 2020.
22. N. Xu, Wang, P., Chen, L., Tao, J., & Zhao, J. Mr-gnn: multi-resolution and dual graph neural network for predicting structured entity interactions, *Proceedings of the 28th International Joint Conference on Artificial Intelligence*, vol. IJCAI, Macau China, 2019.
23. Y. Wang, Min, Y., X Chen, & Wu, J. (2021). Multi-view graph contrastive representation learning for drug-drug interaction prediction, *WWW '21: The Web Conference 2021*, Association for Computing Machinery, Ljubljana, Slovenia, 2021.
24. Chen Y, et al. MUFFIN: multi-scale feature fusion for drug-drug interaction prediction. *Bioinformatics* 2021;**37**(17):2651–8.
25. Asada M, Miwa M, Sasaki Y. Using drug descriptions and molecular structures for drug-drug interaction extraction from literature. *Bioinformatics* 2020;**37**(12):1739–46.
26. Shi J-Y, Mao K-T, Yu H, et al. Detecting drug communities and predicting comprehensive drug-drug interactions via balance regularized semi-nonnegative matrix factorization. *J Chem* 2019;**11**(1):28.
27. Y. Chen, T. Qian, H. Liu, and K. Sun, Bridge: enhanced signed directed network embedding, *CIKM 2018 - Proceedings of the 27th ACM International Conference on Information and Knowledge Management*, Association for Computing Machinery, 2018.
28. V. S. Jonker DM, Van der Graaf PH, Voskuyl RA, et al. Towards a mechanism-based analysis of pharmacodynamic drug-drug interactions in vivo. *Pharmacol Ther* 2005;**106**(1):1–18.
29. Wishart DS, et al. DrugBank 5.0: a major update to the DrugBank database for 2018. *Nucleic Acids Res* 2017;**46**(D1):D1074–82.
30. Rogers D HM. Extended-connectivity fingerprints. *J Chem Inf Model* 2010;**50**(5):742–54.
31. S. Kumar, F. Spezzano, V. Subrahmanian, and C. Faloutsos, Edge weight prediction in weighted signed networks, *IEEE 16th International Conference on Data Mining (ICDM)*, Spain, 2016.
32. Wen YM, Huang L, Wang CD, et al. Direction recovery in undirected social networks based on community structure and popularity. *Information Sciences* 2018;**473**:31–43.
33. J. Kim, H. Park, J. E. Lee, and U. Kang, SIDE: representation learning in signed directed networks, *WWW '21: The Web Conference 2021*, Association for Computing Machinery, Ljubljana, Slovenia, 2021.
34. T. Jie, T. Lou, and J. M. Kleinberg, Inferring social ties across heterogeneous networks, in *Proceedings of the Fifth International Conference on Web Search and Web Data Mining, WSDM 2012*, Seattle, WA, USA, 8–12, 2012, **2012**.
35. Tang J, Chang Y, Aggarwal C, et al. A Survey of Signed Network Mining in Social Media. *ACM Comput Surv* 2015; **49**(3):37.
36. Q. V. Dang and C. L. Ignat, Link-sign prediction in dynamic signed directed networks, in *2018 IEEE 4th International Conference on Collaboration and Internet Computing (CIC)*, 2018.
37. Davis JAJSN. Clustering and structural balance in graphs. *Human Relations*, **20**(2):181–187.
38. Schlichtkrull M, Kipf TN, Bloem P, et al. *Modeling Relational Data with Graph Convolutional Networks*. The Semantic Web, ESWC 2018. Lecture Notes in Computer Science, vol 10843. Springer, Cham.

39. Velikovi P, Cucurull G, Casanova A, et al. Graph Attention Networks. *Conference Track 6th International Conference on Learning Representations, ICLR, Vancouver Canada*, 2018.
40. Huang J, Shen H, Hou L, et al. SDGNN: Learning Node Representation for Signed Directed Networks. *Association for the Advancement of Artificial Intelligence, AAAI, on-line*, 2021.
41. Yan XY, Zhang SW. Identifying drug-target interactions with decision templates. *Curr Protein Pept Sci* 2018;**19**(5): 498–506.
42. Kipf TN, Welling M. Semi-supervised classification with graph convolutional networks. *arXiv:160902907* 2016.
43. Y. Li, Y. Tian, J. Zhang, and Y. Chang, Learning signed network embedding via graph attention, *Proceedings of the AAAI Conference on Artificial Intelligence*, vol. **34**, no. 4, pp. 4772-4779, 2020.
44. Derr T, Ma Y, Tang J. Signed Graph Convolutional Network. *2018 IEEE International Conference on Data Mining, ICDM, Singapore*, 2018.
45. G. Salha, S. Limnios, R. Hennequin, V. A. Tran, and M. Vazirgiannis, Gravity-Inspired Graph Autoencoders for Directed Link Prediction, in the *28th ACM International Conference*, 2019.
46. Zhu S, Li J, Peng H, et al. Adversarial directed graph embedding 2020.